frontiers | Frontiers in Marine Science

TYPE Original Research
PUBLISHED 24 January 2023
DOI 10.3389/fmars.2023.1106663

OPEN ACCESS

EDITED BY
Raden Dwi Susanto,
University of Maryland,
United States

REVIEWED BY
Liang Yi,
Tongji University, China
Xiangzhou Song,
Hohai University, China

*CORRESPONDENCE
Shengfa Liu
liushengfa@fio.org.cn
Xuefa Shi
xfshi@fio.org.cn

SPECIALTY SECTION
This article was submitted to Physical Oceanography, a section of the journal Frontiers in Marine Science

RECEIVED 25 November 2022
ACCEPTED 12 January 2023
PUBLISHED 24 January 2023

CITATION
Liu S, Ye W, Zhang H, Cao P, Li J, Sun X, Li X, Fang X, Khokiattiwong S, Kornkanitnan N and Shi X (2023) Sediment provenances shift driven by sea level and Indian monsoon in the southern Bay of Bengal since the last glacial maximum. *Front. Mar. Sci.* 10:1106663. doi: 10.3389/fmars.2023.1106663

Sediment provenances shift driven by sea level and Indian monsoon in the southern Bay of Bengal since the last glacial maximum

Shengfa Liu[1,2]*, Wenxing Ye[1,3], Hui Zhang[1,2], Peng Cao[1,2], Jingrui Li[2], Xingquan Sun[4], Xiaoyan Li[1,2], Xisheng Fang[1,2], Somkiat Khokiattiwong[5], Narumol Kornkanitnan[5] and Xuefa Shi[1,2]*

[1]Key Laboratory of Marine Geology and Metallogeny, First Institute of Oceanography, Ministry of Natural Resources, Qingdao, China, [2]Laboratory for Marine Geology, Qingdao National Laboratory for Marine Science and Technology, Qingdao, China, [3]College of Marine Geosciences, Ocean University of China, Qingdao, China, [4]Jimo District Bureau of Natural Resources, Qingdao, China, [5]Marine and Coastal Resources Research and Development Institute, Department of Marine and Coastal Resources, Ministry of Natural Resources and Environment, Bangkok, Thailand

The Tibetan Plateau uplift has induced the formation of the largest sediment source-sink system in the northeast Indian Ocean, which has become an ideal region for investigating land-sea interaction processes. However, many questions regarding sediment transport patterns and their controlling factors at different time scales remain unanswered. Therefore, in the present study, a gravity core named BoB-79, based on the southern Bay of Bengal (BoB) was selected to investigate sediment provenance shift and its corresponding mechanism to sedimentary environment change since the last glacial maximum (LGM). The clay mineral compositions are analyzed and the whole core sediments reveal a feature dominated by illite (~55%), followed by chlorite (~24%) and kaolinite (~17%), and the content of smectite (~4%) is the lowest. A trigonometric analysis of provenance discrimination of clay minerals showed that the Himalayas, together with the Indian Peninsula, represent the main sources of southern BoB sediments, and the last glacial period might have been controlled by the dominant Himalayan provenance, with an average contribution of approximately 90%. However, as a secondary source, the influence of the Indian Peninsula increased significantly during the Holocene, and its mean contribution was 24%, thus, indicating that it had a crucial effect on the evolution process of BoB. The sediment transportation pattern changed significantly from the LGM to the Holocene: in the last glacial period, the low sea level exposed the shelf area that caused the Ganges River connected with the largest submarine canyon in BoB named Swatch of No Ground (SoNG), and the Himalayan materials could be transported to the BoB directly under a strong turbidity current, thereby forming the deep sea deposition center with a sedimentation rate of 4.5 cm/kyr. Following Holocene, the sea level increased significantly, and the materials from multiple rivers around the BoB were directly imported into the continental shelf area. The intensive Indian summer monsoon dominated the transportation process of the terrestrial materials,

thereby forming a deposition center in the shallow water area of the continental shelf northeast Indian Ocean; subsequently, the material flux relative to the input to the deep sea area decreased significantly, and the sedimentation rate in the southern BoB decreased to 1.7 cm/kyr.

KEYWORDS

last glacial maximum (LGM), sea level, Indian monsoon, dynamical process, Bay of Bengal (BoB), sedimentary pattern

1 Introduction

Source to sink is an important study topic in modern marine sedimentology research (Goodbred, 2003; Manville et al., 2009; Leithold et al., 2016; Shi et al., 2021). The transportation and sedimentation process of sediments in typical continental margins, the formation and primary control factors of shelf sedimentary systems, and the mechanism of the response of land-sea interactions to climatic and environmental changes are the core scientific issues in this research field (Allen, 2008; Yang et al., 2015; Sebastian et al., 2023). In sediment source-sink systems, rivers play a critical role in material transport processes, land-sea energy balance, and biogeochemical cycles (Gao and Jia, 2004; Selvaraj and Chen, 2006; Liu et al., 2008; Shi et al., 2015). Coupling studies on river-shelf systems have also become one of the hot topics in marine sedimentology research (Galy and France-Lanord, 1999). Therefore, a profound understanding of the material flux and composition characteristics of rivers entering the sea, the transportation of materials, material burial and circulation processes from the rivers to the marginal sea and the global ocean, and their responses to global climatic changes at different scales is very crucial to further elucidate land-sea interaction mechanisms and material balance of payments. This knowledge can also serve as appropriate reference materials for research on global changes in different latitudes and climate zones and further provide a theoretical basis for reconstructing past environmental and climate evolution.

The Tibetan Plateau uplift is globally the largest sediment source-sink system in the northeast Indian Ocean (Gaillardet and Galy, 2008; Ding et al., 2022). The BoB is the world's largest bay in the northeastern Indian Ocean, and it is also one of the primary sinks for the seaward material transport from the Himalayas and the Tibetan Plateau, with the development of large deltas, shelves, slopes, submarine canyons, and deep-sea fan sedimentary systems (Curray and Moore, 1974; Curray et al., 2003). The abundant material supply of the BoB, the formation of large rivers, the multiple topographic types, and the typical monsoon climate make BoB the best natural laboratory to investigate land-sea interactions. The differences in geological background, climatic belt, biological ecosystems, and human activities among rivers such as Krishna-Godavari (K-G), Ganges-Brahmaputra (G-B), Mahanadi (M), and Irrawaddy (I) rivers distributed around the BoB have led to different compositions of the terrestrial sediments transported by these rivers into the sea (Colin et al., 1999; Tripathy et al., 2011; Tripathy et al., 2014; Joussain et al., 2016); this enables to quantitatively identify sediment contributions from complex multisource sediments from different provenances in the BoB. The BoB is located in a typical Indian monsoon region with distinct dry and wet seasons. The changes in the intensity of the Indian monsoon, especially the summer wind, play a critical role in the physical erosion, chemical weathering, and sediment transportation of the sediment provenance regions (Liu et al., 2020). Because of a unique climate and dynamic transport conditions, the distribution and contribution of marine sediments from different provenances have remarkable spatial and temporal differences. These differences contribute to understanding variations in past climate and hydrodynamic environments within a particular study area. Therefore, from a scientific perspective, it is very critical to find appropriate alternative indicators to clarify the temporal and spatial differences in the distribution and contribution of materials from different provenances in the ocean, interpret the climatic and environmental signals, and reveal their control mechanisms.

Sediment provenance in the BoB has been suggested to be mostly terrestrial detritus material, and the contribution of marine autogenous organic matter, wind dust, and volcanic material are relatively small (Weber et al., 2003; Tripathy et al., 2014; Li et al., 2018; Li et al., 2019; Ye et al., 2022). Recent studies have shown that the contribution of materials from Indian rivers to the BoB is >20% (Sun et al., 2019; Sun et al., 2020); however, it remains unclear how this material from different river sources has changed over a historical period. To date, few studies have been conducted on this topic. Therefore, in this study we comprehensively analyze the characteristics of clay minerals in core BoB-79 sediments from the southern BoB, quantitatively identifies the contribution of materials from different river provenances, reveals the response of sediment provenance changes to sea level fluctuations and Indian monsoon since the last glacial maximum, further to discuss the transport pattern and control mechanism of sediments at different times.

2 Materials and methods

2.1 Sample collection

A China-Thailand joint investigation cruise collected samples from one gravity core, namely BoB-79 (location: 9.96°E, 87.97°N; length: 1.67 m; water depth: 3427 m), in March 2014 (Figure 1). To

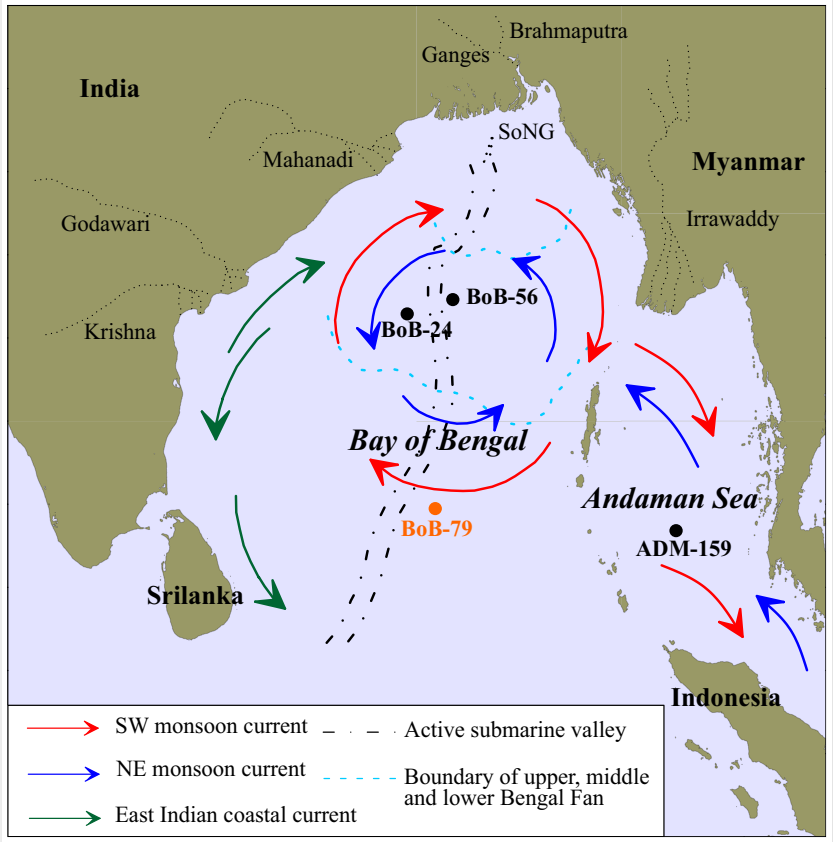

FIGURE 1
Location of the core BoB-79 sediment and the related reference cores BoB-24 (Ye et al., 2022), BoB-56 (Li et al., 2018), and ADM-159 (Liu et al., 2020; Liu et al., 2021a) in the northeastern Indian Ocean. Ocean dynamic conditions driven by seasonal monsoons are presented by different color arrows, and the active submarine valley crossing the whole BoB is shown by the black dotted line. SoNG is presented by black dotted line (Curray et al., 2003; Chauhan and Vogelsang, 2006).

comprehensively analyze the samples, this work collected 167 sub-samples from the core at 1 cm interval.

2.2 AMS ^{14}C analysis

The radiocarbon age of the shells of the planktonic foraminifera *Globorotalia menardii* from nine typical layers was measured by the Accelerator Mass Spectrometry (AMS) method. The radiocarbon age was corrected for a local reservoir age of –60 ± 51 years (Dutta et al., 2001) and converted to calendar age (1σ errors) by using Calib Rev 7.0.4 (Reimer et al., 2013). The shells of the foraminifera were pretreated at the Key Laboratory of Marine Geology and Metallogeny, Ministry of Natural Resources, China, and AMS^{14}C analyses were performed at the Beta Analytic Laboratory, USA.

2.3 Grain size analysis

The pretreatment of the samples for grain size analysis was performed as follows: a 15 mL H_2O_2 solution (30%) was added to remove organic matter from the shells, and the samples were then bathed in a 5 mL HCl solution (3 mol/L) for 24 h to remove calcareous cement and shell materials. All samples were fully desalted and dispersed before conducting the measurements. By using the Mastersizer 3000 instrument (Malvern Ltd., UK; resolution, 0.01 Φ; measurement range, 0.02–2000 μm), sample grain sizes were assessed in the Key Laboratory of Marine Geology and Metallogeny, Ministry of Natural Resources, China. After repeated measurements, the experimental error was predicted to be<3%. For data processing, the moment method was used for calculating grain size parameters, including sorting coefficient, mean grain size, kurtosis, and skewness (McManus, 1988).

2.4 Clay mineral analysis

X-ray diffraction (XRD) was conducted to identify clay-sized particles (<2 μm). Subsequently, the samples were treated with 30% H_2O_2 to remove organic matter and then with 1 M HCl to remove calcium carbonate. The samples were then rinsed continuously with distilled water until deflocculation occurred. In accordance with Stokes' law, particles<2 μm in size were collected, sedimented, and centrifuged for determination. XRD was performed in three cycles in the 24-h air drying and ethylene glycol solvation condition, followed by heating for another 2 h at 490°C. Under CuK-α radiation, the D/Max 2500 PC diffractometer was used for obtaining XRD graphs at 100 mA intensity and 40 kV voltage. In the present study, diffraction patterns (2θ) were scanned in the range of 3°–30° at the 0.02° step size. Clay minerals were mostly identified based on

(001) series of the basal reflection position observed from 3 XRD graphs for kaolinite+chlorite at 0.7 nm and illite at 1 nm together with smectite at 1.7 nm. Chlorite and kaolinite were separated according to their relative proportions based on the 0.357/0.354 nm peak ratio. By using Biscaye's method (Biscaye, 1965), the intensity factors for kaolinite+chlorite, illite, and smectite were 2, 4, and 1, respectively. The error for the relative clay material level was predicted as <10%.

3 Results

3.1 Chronology and AMS ^{14}C age model

In the present study, the BoB-79 core age model was constructed by linearly interpolating the ^{14}C age data, and the entire core sediments covered the sequential record over the last 43.5 cal ka BP (Figure 2). The recently updated algorithm COPRA (Breitenbach et al., 2012) was used to optimize the BoB-79 age model for interpreting age uncertainty applied in determining proxy error estimates. The core deposition rate of BoB-79 was relatively stable, with an average sedimentation rate of approximately 3.8 cm/kyr; the core sedimentation rate had increased in the last glacial period as compared to that in the Holocene (approximate average: 4.5 cm/kyr vs. 1.7 cm/kyr).

3.2 Lithology and grain size composition

The lithology of BoB-79 core sediment showed relative heterogeneity, with mostly gray-brown silt, while the sediment tended to have a dark color from top to bottom (Figure 3). According to the changes in sediment lithology, the entire core was classified into upper and lower sections at 38 cm: the 0–38 cm section was yellow-brown silt, and no apparent layering change was observed. There were two dark interlayers distributed at 21–23 cm and 32–34 cm. The layer at 38–167 cm had gray-brown silt with a uniform lithology and no apparent stratigraphic changes; the water content and viscosity of the sediment in this section were lower than those in the 0–38 cm section.

The grain size results of BoB-79 core sediments showed the highest composition of silt, with an average of 68.5%, followed by clay components (14.7%–41.7%); the content of sand components was the lowest (range: 0.3%–17.2%). The variations in the characteristics of grain size composition and parameters (sorting coefficient, mean grain size, kurtosis, and skewness) of the core sediment could be roughly divided into two sections with 38 cm as the boundary. The detailed characteristics are described as follows.

In the bottom section (38–167 cm): the content of sand components was 0.27%–11.07%, with an average of 5.35%. The contents of silt sand components and clay components were 56.30%–84.14% and 14.70%–41.66%, respectively, with an average of 69.39% and 25.26%, respectively. The particle size range was 6.52–7.77Φ, with an average of 6.98Φ. The sorting coefficient was 1.32–1.93, and the sorting performance was poor. The range of the skewed state was −1.56 to 1.16; the sediments at this stage were mainly negatively skewed, and the positively biased sediments appeared only in individual layers. The peak state was 1.77–2.56, with a wide range of peak states. Apparent fluctuations were noted in each particle size parameter.

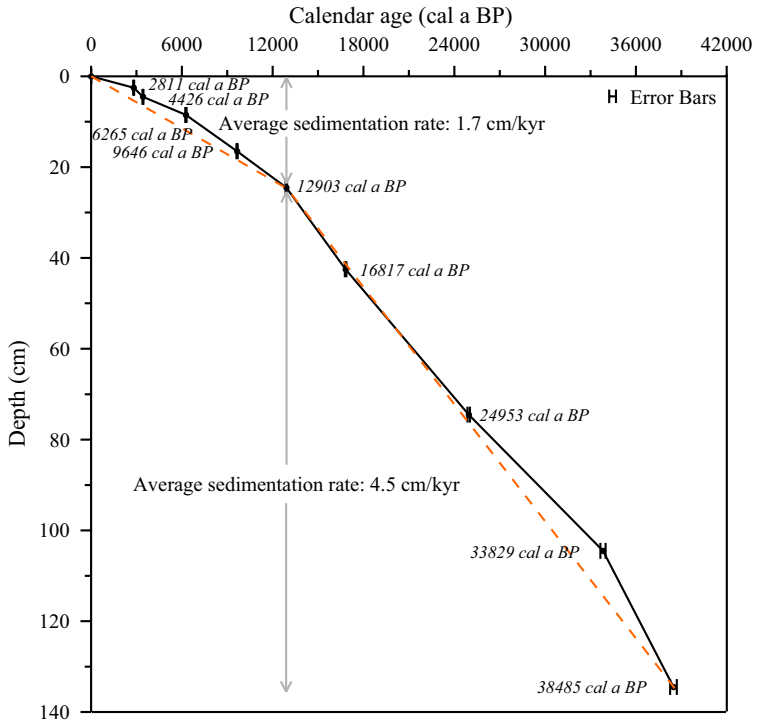

FIGURE 2
The AMS^{14}C age model of the core BoB-79 and the calculated average sedimentation rate since the last glacial period; error bars represent the uncertainty of each dating point.

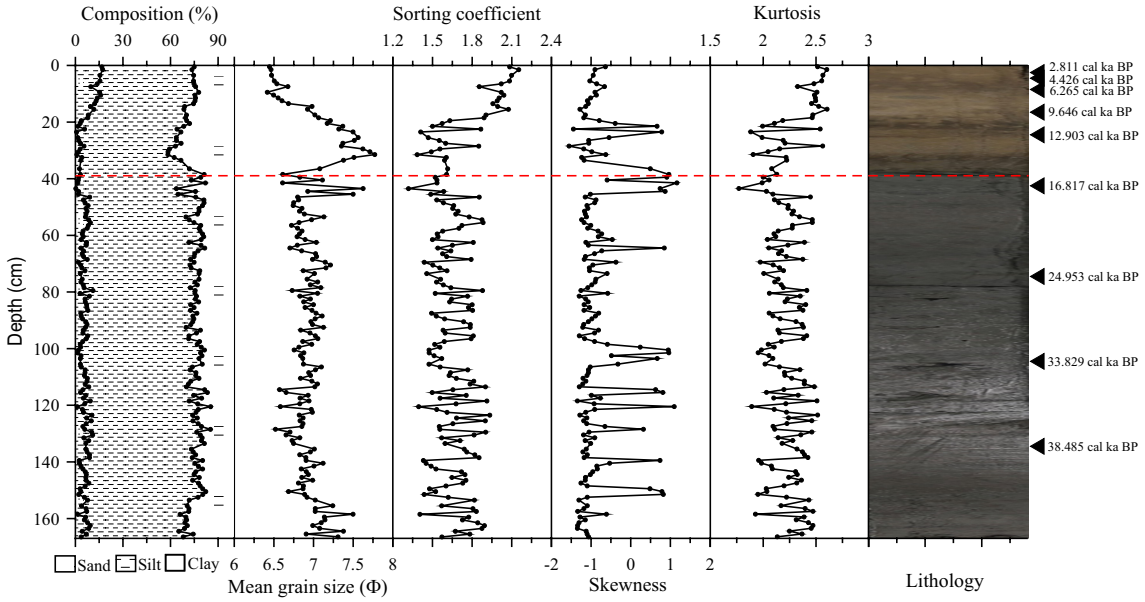

FIGURE 3
Vertical distribution of sediment grain size parameter and sediment lithology from the core BoB-79; the red dotted line represents the boundary of the two stratum units, black triangles show the AMS^{14}C data point.

The top section (0–38 cm): The content of sand grade components was 3.03%–17.21%, with an average of 11.92%. The contents of silt sand components and clay components were 56.30%–68.98% and 22.22%–31.56%, respectively, with an average of 61.39% and 26.69%, respectively. The particle size range was 6.42–7.21Φ, with an average of 6.72Φ. The sorting coefficient was 1.57–2.51, and the sorting performance was poor to very poor. The skewed state was –1.28 to –0.39, all of which were negatively skewed. The peak state was 2.11–2.60, which indicated a wide range of peak state width. Each particle size parameter was stable within the range of their respective maximum/minimum values after consistent increase/decrease at this stage.

3.3 Clay mineral composition

Four main clay minerals in BoB-79 core sediments, together with changes of illite chemical weathering index and illite crystallinity, are shown in Figure 4. Illite showed the highest content (range: 43%–65%, mean: 55%), followed by chlorite (range: 15.14%–32.57%, mean: 24%); kaolinite and smectite exhibited lower contents, with an average content of 17% and 5% and ranges of 14%–22% and 0–16%, respectively.

Regarding the trend in clay mineral change, two stratum units could also be identified with the boundary of 38 cm. Illite and chlorite had higher content in the bottom stratum unit (38–167 cm) and showed fluctuations in the relatively high-value zone; the average value in this section was 56% and 25%, respectively. However, the changing trend of these two components at this stratum unit roughly manifested as a “mirror” form, the increase of illite was often accompanied by a decrease in chlorite content. The contents of kaolinite and smectite ware low and stable in this section, with the average content of 17% and 3%, respectively. In the top stratum unit (0–38 cm), both illite and chlorite showed a decreasing trend, with new averages of 48% and 22%, respectively. Kaolinite and smectite remained high after a rapid increase at 20 cm, the average content of kaolinite and smectite was 20% and 10% in this section, respectively.

The chemical weathering index of illite ranged between 0.31 and 0.95, and the fluctuation change in the bottom stratum unit showed a decrease trend upward. The crystallinity of illite was 0.23–0.48, and there was no apparent change in the whole core sediment.

4 Discussion

4.1 Sediment provenance discrimination based on clay mineral proxy

As an important component of fine fraction sediments, clay minerals are extensively present in marine sediments, and they show a high sensitivity to marine geological processes and sedimentary environments (Dou et al., 2010; Liu et al., 2012; Qiao et al., 2015; Shi et al., 2015). Because clay minerals are embedded in fine particulate matter, they can be transported in the ocean with suspended bodies over long distances and remain unaltered before entering the sea; this aspect makes the combined characteristics of clay minerals an effective indicator for identifying material sources and tracking sediment transport processes in marine sedimentology research (Xu et al., 2014; Shi et al., 2015; Sun et al., 2020). Previous studies have shown that clay mineral assemblages in sediments from rivers entering the sea around the northern Indian Ocean (Khan et al., 2019) show significant differences; this feature can be used to identify the sediment material source in the BoB (Sun et al., 2020). Therefore, we constructed an illite-smectite-(chlorite+kaolinite) end trigonogram to identify the sediment source in the southern BoB since the LGM by comparing the clay mineral composition of the

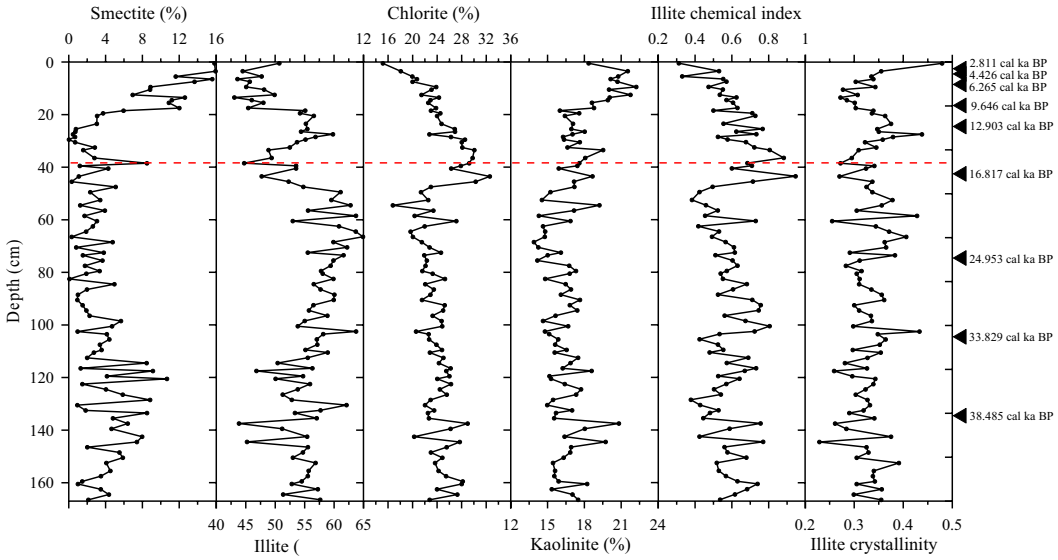

FIGURE 4
Vertical distribution of clay mineral composition, illite chemical index, and illite crystallinity from the core BoB-79; the red dotted line represents the boundary of the two stratum units, black triangles show the AMS^{14}C data point.

BoB-79 core sediment and the surrounding potential source regions (Figure 5); this method has been successfully used for source discrimination in the Indo-Pacific intersection regions (Shi et al., 2015; Ye et al., 2022).

As shown in Figure 5, the coverage areas of the last glacial and Holocene phases were significantly separated, thus, indicating the different sediment sources of these two stages. The BoB-79 sediments had very low smectite content during the last glacial phase, while illite was the dominant mineral. As noted from the trigonogram, the clay mineral assemblage at this time almost completely settled in the Ganges-Brahmaputra River range, thus, indicating that the sediment source at this time was a single source dominated by the Himalayan materials. After entering the Holocene, the BoB-79 core sediments were still closest to the Ganges-Brahmaputra sediment drop, but the smectite content increased significantly during this period. Subsequently, the clay mineral settlement moved toward the Godavari-Krishna and Irrawaddy rivers and were closer to the Indo-Peninsular rivers; hence, we believe that the Indian Peninsula as a secondary source area had a substantial effect on the BoB-79 core sediments at this stage. It should be noted that the sediment clay

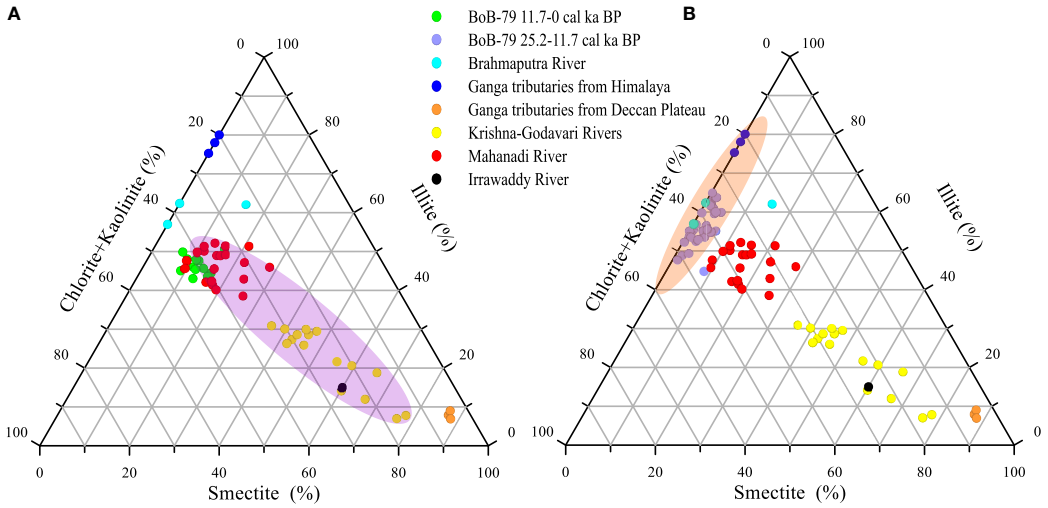

FIGURE 5
Provenance identification of the sediment from the core BoB-79 based on clay mineral composition. Two stages (25.2–11.7 cal ka BP and 11.7–0 cal ka BP) sediment clay mineral results from the core BoB-79 are compared with the tentative sediment provenance regions of Brahmaputra River (Datta and Subramanian, 1997), Ganga tributaries from the Himalayan region (Sarin et al., 1989), Ganga tributaries from the Deccan Plateau (Sarin et al., 1989), Krishna-Godavari Rivers (Phillips et al., 2014), Mahanadi River (Phillips et al., 2014), and Irrawaddy River (Rodolfo, 1969). The gray shades represent sediments from the Himalayas **(B)** and the Indian Peninsula **(A)**, respectively.

mineral drop points in both stages were distant from the Irrawaddy River material, thus, suggesting that the material contribution from this river into the sea on the eastern side of the BoB could be negligible. Gravity core sediments, namely BoB-24 and BoB-56, in the central BoB also showed significant changes in the last glacial and Holocene material sources (Li et al., 2018; Ye et al., 2022); however, the timing of this transition was not consistent, which mainly reflects the difference in the deposition process of the different spatial locations, southern core sediment presented an earlier response to sea level rising than that in the central BoB. The core sediment investigated in the present study was located in the southern BoB, which belongs to the distal sink of the terrestrial material, and its deposition environment is relatively stable; this finding indicates the sedimentary pattern of the southern BoB and its primary controlling mechanism.

From the above source identification results, we selected the Himalayan and Indian peninsula source areas as the two main end elements of BoB-79 core sediments, with Ganges-Brahmaputra rivers and Krishna-Godavari rivers being the representatives, respectively, using clay minerals to combine smectite and illite+kaolinite levels. The relative contribution ratio of the two source areas was calculated according to the following equilibrium equation:

$$5X_i + 58Y_i = S_i \quad (1)$$

$$85X_i + 39Y = IK_i \quad (2)$$

In the formula, X_i and Y_i represent the contribution ratios of Himalayan and Indian source areas to the BoB-79 sediment, respectively. S_i and IK_i represent smectite and illite+kaolinite percentage contents in sample i, respectively, and the coefficients on the left of the equation represent the mean corresponding clay mineral combination contents of these two source areas, respectively (Sarin et al., 1989; Phillips et al., 2014).

The results revealed that the source of sediment in the BoB has been in the process of constant alteration after the last glacial period (Figure 6). The contribution of the Himalayan source area in the last glacial period was approximately 90%; this contribution significantly reduced in the Holocene period, with an average contribution of 76%. Correspondingly, the average contribution of the Indian source region in the last glacial period was approximately 10%, and it exhibited a clear increasing trend after entering the Holocene period, with an average contribution of 24%. Modern sediment source discrimination in the BoB also shows that Indian source material is mainly deposited on the west side of the BoB, and its main transport force is the seasonal monsoon flow (Li et al., 2017; Sun et al., 2019; Sun et al., 2020), the results of this study show that the inflow of materials from rivers such as the Godavari-Krishna River can be transported over long distances to the south, which plays an important role in the formation and evolution of turbidity fans in the BoB.

4.2 Sedimentary pattern of the BoB after the LGM

Significant changes in the global climate after the LGM are clearly recorded in northern Indian Ocean sediments, where monsoon intensity, land-sea interactions, and ocean productivity show good remote correlations with high latitudes (Andersen et al., 2006; Rasmussen et al., 2006; Liu et al., 2021b). Based on the identification results of clay minerals, the BoB-79 core sediment in the southern BoB was a single Himalayan source during the last glacial period, and its contribution was approximately 90%. The Holocene period witnessed a mixed source of Himalayan and Indian source areas, among which the Himalayan source area was the primary source area that contributed approximately 80%, with the Indian peninsula acting as a secondary source area and contributing approximately 20%. From the last glacial period to the Holocene period, significant changes occurred in the sea level, leading to changes in the marine sedimentary environment in the southern BoB; moreover, significant changes in climatic conditions from the last glacial period to the Holocene period have led to changes in sediment transport forces and ultimately patterns of sediment formation (Liu et al., 2021a; Ye et al., 2022; Sebastian et al., 2023).

During the last glacial period, the sea levels decreased, especially in the LGM period, the sea level was approximately 120 m lower than the present level (Fairbanks, 1989; Chappell, 2002; Cutler et al., 2003; Arz et al., 2007) (Figure 6). The northern shelf of the BoB is exposed, the estuary extends seaward, and the northern SoNG receives sediments transported into the sea from the Ganges-Brahmaputra rivers (Curray et al., 2003; Li et al., 2019). A sufficient supply of sediments causes strong turbidity in the active submarine canyon, and massive sediments from the Himalayas are delivered to the deep sea through turbidity; moreover, the overflow waterway is deposited on the surface of the BoB during transportation (Kuehl et al., 1989; Curray et al., 2003). Turbidity and its overflow were the main drivers of the transport of terrestrial detritus material to the BoB during this period. The BoB-79 core is located in the eastern part of the SoNG, and it is affected by turbidity overflow. The channel-levee system formed by turbidity current along the seafloor has continuously transported sediments from rivers and the shelf to the deep sea over geological history, forming the characteristic deep-sea turbidite layers (Weber and Reilly, 2018; Fauquembergue et al., 2019; Li et al., 2021). The last glacial stage had a high sedimentation rate (mean: 4.5 cm/kyr), and the ratio of smectite to illite in this stage was stabilized in the low range of vibration, thus, indicating the control of materials from the Himalayan source area. The quantitative calculation results also showed that the Himalayan source area contributed more than 90% during this period (Figure 6), and the deposition center was formed in the BoB (Figure 7). Because of the lack of huge submarine canyons in the Indian peninsula, the estuary of the river is disconnected from the BoB, and sediments cannot be transported to the sea in large quantities; moreover, a very small amount of material entering the sea mainly relies on the transport of surface circulation. The flux of the river is also significantly smaller than that of the Ganges-Brahmaputra rivers; thus, even if few sediments are delivered to the deep waters of the BoB, their source signal is masked by the Himalayan material.

After entering the Holocene period, there was a rapid increase in sea levels to above –60 m, and the northern shelf was gradually submerged by seawater (Contreras-Rosales et al., 2014). The direct link between the SoNG and the Ganges-Brahmaputra rivers was cut off (Curray and Moore, 1971), and more sediments were captured by the shelf, thus, forming a deposition center in the shelf area (Figure 7).

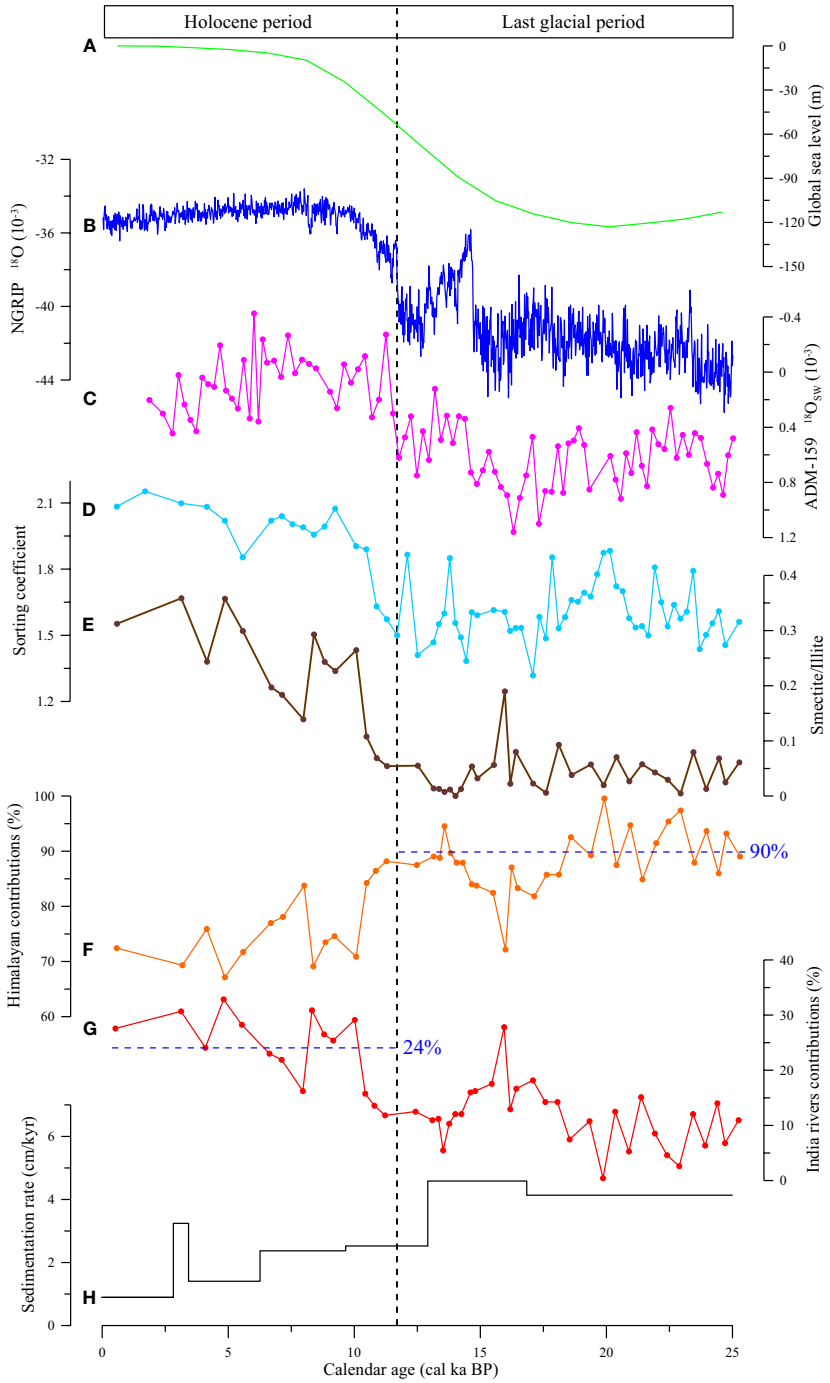

FIGURE 6
Contributions of different provenances and comparison against the related records for the northern Indian Ocean since the LGM. **(A)** Relative global sea level estimates based on corals (Waelbroeck et al., 2002); **(B)** Greenland NGRIP ice core oxygen isotope composition (Andersen et al., 2006; Rasmussen et al., 2006); **(C)** Sea water oxygen isotope composition of the core ADM-159 in the central Andaman Sea (Liu et al., 2021a); **(D)** Sediment sorting coefficient of the core BoB-79 (present study); **(E)** Ratio of smectite and illite of the core BoB-79 (present study); **(F)** Contributions of Himalayan provenance (present study); **(G)** Contributions of India river provenance (present study); **(H)** sedimentation rate calculated based on the AMS^{14}C data of the core BoB-79 (present study). 90% and 24% present the average contributions from Himalayas and Indian Peninsula, respectively.

The sedimentary environment during this period also caused insufficient sediment supply to the BoB, thereby weakening the turbidity activity. Turbidity and its overflow occurred only in the northern and central BoB, thus, making it difficult to affect the southern BoB where the BoB-79 core is located (Curray et al., 2003; Weber et al., 2003; Weber and Reilly, 2018); this also became a watershed for changes in the sediment source area of the study area. Consequently, clay mineral provenance was identified. Holocene sediments remained closest to Ganges-Brahmaputra sediment drop, but smectite content increased significantly during this period. As shown in Figure 5, the clay mineral plots moved toward the rivers of the Indian Peninsula. The intensity of the early Holocene Indian

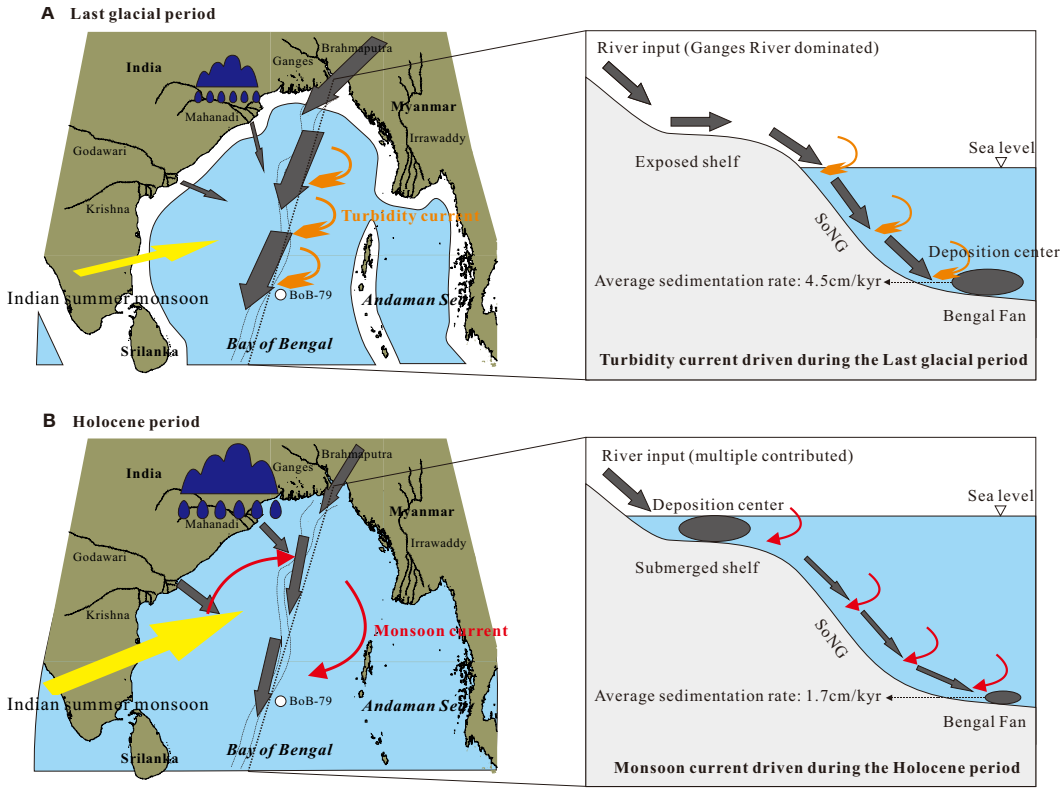

FIGURE 7
Sedimentary pattern of Bengal fan during the last glacial period **(A)** and the Holocene period **(B)**, the size of grey arrows presents the relative contributions of different material prevenances, color arrows represent Indian summer monsoon, monsoon current and turbidity current in the BoB, black ellipses show deposition center at the Bengal Fan during the last glacial period and submerged shelf during the Holocene.

summer monsoon was significantly enhanced, and the climate was warmer and wetter than that in the LGM (Liu et al., 2021a). The remarkably elevated smectite content in the Holocene period may be caused by changes in the climate environment (Cao et al., 2015). However, the chemical index of illite decreased during this period, and the crystallinity of illite improved (Figure 4); this finding was inconsistent with the trend of climate shifting toward warm and moist conditions, thus, indicating that the increase in smectite in BoB-79 during the Holocene period reflects a change in sediment provenance. The significant increase in the sorting coefficient during the Holocene period (Figure 3) also indicates that the sediments at this stage were likely to be from mixed sources. Based on the qualitative identification of clay minerals, the secondary source area after entering the Holocene period should be the Indian Peninsula material. In the Holocene phase, because of the absence of turbidity activity in the BoB, the monsoon-driven surface circulation system was the predominant movement factor for sediment transport in the southern BoB; this obviously greatly reduced the supply of the Himalayan material to the study area, as confirmed by the significant decline in the deposition rate during the Holocene period. The results of quantitative calculations revealed that the relative contribution of the Indian source areas increased significantly by more than 20% during the Holocene period (Figure 6), mainly because of the reduction in the material supply from the Himalayas.

5 Conclusions

In the present study, clay mineral characteristics from BoB-79 sediments in the southern BoB were comprehensively analyzed, and the source identification of the fine-grained sediment was performed using the illite-smectite-(chlorite+kaolinite) end trigonogram. The Himalayas and the Indian peninsula represent the two major sediment sources in southern waters from the BoB, among which the last glacial stage was controlled by a single Himalayan source; the influence of the Indian source area as a secondary source increased significantly in the Holocene period. Based on the quantification results, the Himalayan source area in last glacial stage had a mean contribution of 90%, while that in the Holocene stage was 76%. Correspondingly, the average contribution of the Indian source area during the last glacial phase was 10% and 24%, respectively, during the Holocene period.

Controlled by sea level elevation, the transportation of sediments within our study area changed remarkably from last glacial to the Holocene period. The low sea level and frequent turbidity flow activity during the last glacial period were the main driving forces for the transportation of the terrestrial detritus material to the BoB, mainly transporting erosion products from the Himalayas to the study area with the sedimentation rate as high as 4.5 cm/kyr. After entering the Holocene period, the sea level increased significantly, the turbidity activity weakened and these conditions no longer affected the southern BoB, while the surface circulation system driven by the

Indian summer monsoon became the predominant factor of sediment delivery to the BoB. The material supply in the Himalayan source area decreased significantly, the sedimentation rate decreased to 1.7 cm/kyr, and the relative material contribution from the Indian peninsula as the secondary source area increased.

Data availability statement

The raw data supporting the conclusions of this article will be made available by the authors, without undue reservation.

Author contributions

SL and XS were responsible for study conception. WY, XS, PC, and HZ contributed to sample pretreatment and measurement. The authors interpreted the data and wrote the manuscript together. All authors contributed to the article and approved the submitted version.

Funding

This work was supported by National Programme on Global Change and Air-Sea Interaction (GASI-04-HYDZ-02), National Natural Science Foundation of China (42176089, 41676054), Taishan Scholar Program of Shandong (tspd20181216), China-ASEAN blue partnership construction program, and China-Thailand cooperation project "Research on Vulnerability of Coastal Zones.

Acknowledgments

We would like to thank the crew of M.V. SEAFDEC, the staff from Phuket Marine Biological Center, Ministry of Natural Resources and Environment, Thailand, and First Institute of Oceanography, Ministry of Natural Resources, China for sediment sampling on board. This work was supported by National Programme on Global Change and Air-Sea Interaction (GASI-04-HYDZ-02), National Natural Science Foundation of China (42176089, 41676054), Taishan Scholar Program of Shandong (tspd20181216), China-ASEAN blue partnership construction program, and China-Thailand cooperation project "Research on Vulnerability of Coastal Zones".

Conflict of interest

The authors declare that the research was conducted in the absence of any commercial or financial relationships that could be construed as a potential conflict of interest.

Publisher's note

References

Allen, P. A. (2008). From landscapes into geological history. *Nature* 451 (7176), 274–276. doi: 10.1016/S0264-8172(03)00035-7

Andersen, K. K., Svensson, A., Johnsen, S. J., Rasmussen, S. O., Bigler, M., Röthlisberger, R., et al. (2006). The Greenland ice core chronology 2005, 15-42 ka. Part 1: Constructing the time scale. *Quaternary Sci. Rev.* 25, 3246–3257. doi: 10.1016/j.quascirev.2006.08.002

Arz, H. W., Lamy, F., Ganopolski, A., Nowaczyk, N., and Pätzold, J. (2007). Dominant northern hemisphere climate control over millennial-scale glacial sea-level variability. *Quaternary Sci. Rev.* 26, 312–321. doi: 10.1016/j.quascirev.2006.07.016

Biscaye, P. E. (1965). Mineralogy and sedimentation of recent deep-sea clay in the Atlantic ocean and adjacent seas and oceans. *GSA Bull.* 76, 803–832. doi: 10.1130/0016-7606(1965)76[803:MASORD]2.0.CO;2

Breitenbach, S. F. M., Rehfeld, K., Goswami, B., Baldini, J., and Marwan, N. (2012). Constructing proxy records from age models (COPRA). *Climate Past* 8 (5), 1765–1779. doi: 10.5194/cp-8-1765-2012

Cao, P., Shi, X. F., Li, W. R., Liu, S. F., Yao, Z. Q., Hu, L. M., et al. (2015). Sedimentary responses to the Indian summer monsoon variations recorded in the southeastern Andaman Sea slope since 26 ka. *J. Asian Earth Sci.* 114, 512–525. doi: 10.1016/j.jseaes.2015.06.028

Chappell, J. (2002). Sea Level changes forced ice breakouts in the last glacial cycle: New results from coral terraces. *Quaternary Sci. Rev.* 21, 1229–1240. doi: 10.1016/S0277-3791(01)00141-X

Chauhan, O. S., and Vogelsang, E. (2006). Climate induced changes in the circulation and dispersal patterns of the fluvial sources during late quaternary in the middle Bengal fan. *J. Earth System Sci.* 115, 379–386. doi: 10.1007/BF02702050

Colin, C., Turpinb, L., Bertauxc, J., Desprairies, A., and Kissel, C. (1999). Erosional history of the Himalayan and burman ranges during the last two glacial-interglacial cycles. *Earth Planetary Sci. Lett.* 171, 647–660. doi: 10.1016/S0012-821X(99)00184-3

Contreras-Rosales, L. A., Jennerjahn, T., Tharammal, T., Meyer, V., Lückge, A., Paul, A., et al. (2014). Evolution of the Indian summer monsoon and terrestrial vegetation in the Bengal region during the past 18 ka. *Quaternary Sci. Rev.* 102, 133–148. doi: 10.1016/j.quascirev.2014.08.010

Curray, J. R., Emmel, F. J., and Moore, D. G. (2003). The Bengal fan: Morphology, geometry, stratigraphy, history and processes. *Mar. Petroleum Geology* 19 (10), 1191–1223.

Curray, J. R., and Moore, D. G. (1971). Growth of the Bengal deep-sea fan and denudation in the Himalayas. *Geological Soc. America Bull.* 82 (3), 563–572. doi: 10.1130/0016-7606(1971)82[563:GOTBDF]2.0.CO;2

Curray, J. R., and Moore, D. G. (1974). *Geology of continental margins* (New York: Springer Berlin Heidelberg).

Cutler, K. B., Edwards, R. L., Taylor, F. W., Cheng, H., Adkins, J., Gallup, C. D., et al. (2003). Rapid sea-level fall and deep-ocean temperature change since the last interglacial period. *Earth Planetary Sci. Lett.* 206, 253–271. doi: 10.1016/S0012-821X(02)01107-X

Datta, D. K., and Subramanian, V. (1997). Texture and mineralogy of sediments from the Ganges-Brahmaputra-Meghna river system in the Bengal basin, Bangladesh and their environmental implications. *Environ. Geology* 30 (3-4), 181–188. doi: 10.1007/s002540050145

Ding, L., Kapp, P., Cai, F. L., Garzione, C. N., Xiong, Z. Y., Wang, H. Q., et al. (2022). Timing and mechanisms of Tibetan plateau uplift. *Nat. Rev. Earth Environ.* 3, 652–667. doi: 10.1038/s43017-022-00318-4

Dou, Y. G., Yang, S. Y., Liu, Z. X., Clift, P. D., Yu, H., Berne, S., et al. (2010). Clay mineral evolution in the central Okinawa trough since 28 ka: Implications for sediment provenance and paleoenvironmental change. *Palaeogeography Palaeoclimatology Palaeoecol.* 288, 108–117. doi: 10.1016/j.palaeo.2010.01.040

Dutta, K., Bhushan, R., and Somayajulu, B. (2001). Delta r correction values for the northern Indian ocean. *Radiocarbon* 43, 6. doi: 10.1017/S0033822200038376

Fairbanks, R. G. (1989). A 17,000-year glacio-eustatic sea level record: Influence of glacial melting rates on the younger dryas event and deep-ocean circulation. *Nature* 342, 637–642. doi: 10.1038/342637a0

Fauquembergue, K., Fournier, L., Zaragosi, S., Bassinot, F., Kissel, C., Malaizé, B., et al. (2019). Factors controlling frequency of turbidites in the Bengal fan during the last 248 kyr cal BP: Clues from a presently inactive channel. *Mar. Geology* 415, 105965. doi: 10.1126/science.1159279

Gaillardet, J., and Galy, A. (2008). Himalaya-carbon sink or source? *Science* 320 (5884), 1727–1728.

Galy, A., and France-Lanord, C. (1999). Weathering processes in the Ganges–Brahmaputra basin and the riverine alkalinity budget. *Chem. Geology* 159 (1-4), 31–60. doi: 10.1016/S0009-2541(99)00033-9

Gao, S., and Jia, J. J. (2004). Sediment and carbon accumulation in a small tidal basin: Yuehu, Shandong Peninsula, China. *Regional Environ. Change* 4 (1), 63–69. doi: 10.1007/s10113-003-0064-5

Goodbred, S. L. (2003). Response of the Ganges dispersal system to climate change: A source-to-sink view since the last interstade. *Sedimentary Geology* 162 (1-2), 83–104. doi: 10.1016/S0037-0738(03)00217-3

Joussain, R., Colin, C., Liu, Z. F., Meynadier, L., Fournier, L., Fauquembergue, K., et al. (2016). Climatic control of sediment transport from the Himalayas to the proximal NE Bengal fan during the last glacial-interglacial cycle. *Quaternary Sci. Rev.* 48, 1–16. doi: 10.1016/j.quascirev.2016.06.016

Khan, M. H. R., Liu, J. G., Liu, S. F., Seddique, A. A., Cao, L., and Rahman, A. (2019). Clay mineral compositions in surface sediments of the Ganges-Brahmaputra-Meghna river system of Bengal basin, Bangladesh. *Mar. Geology* 412, 27–36. doi: 10.1016/j.margeo.2019.03.007

Kuehl, S. A., Hariu, T. M., and Moore, W. S. (1989). Shelf sedimentation off the Ganges-Brahmaputra river system: Evidence for sediment bypassing to the Bengal fan. *Geology* 17 (12), 1132–1135. doi: 10.1130/0091-7613(1989)017<1132:SSOTGB>2.3.CO;2

Leithold, E. L., Blair, N., and Wegmann, K. W. (2016). Source-to-sink sedimentary systems and global carbon burial: A river runs through it. *Earth-Science Rev.* 153, 30–42. doi: 10.1016/j.earscirev.2015.10.011

Li, J. R., Liu, S. F., Shi, X. F., Feng, X. L., Fang, X. S., Cao, P., et al. (2017). Distributions of clay minerals in surface sediments of the middle bay of Bengal: source and transport pattern. *Continental Shelf Res.* 145, 59–67. doi: 10.1016/j.csr.2017.06.017

Li, J. R., Liu, S. F., Shi, X. F., Zhang, H., Fang, X. S., Cao, P., et al. (2019). Sedimentary responses to the sea level and Indian summer monsoon changes in the central bay of Bengal since 40 ka. *Mar. Geology* 415, 105947. doi: 10.1016/j.margeo.2019.05.006

Li, J. R., Liu, S. F., Shi, X. F., Zhang, H., Fang, X. S., Chen, M.-T., et al. (2018). Clay minerals and Sr-Nd isotopic composition of the bay of Bengal sediments: Implications for sediment provenance and climate control since 40 ka. *Quaternary Int.* 493, 50–58. doi: 10.1016/j.quaint.2018.06.044

Li, J. R., Shi, X. F., Liu, S. F., Qiao, S. Q., Zhang, H., Wu, K. K., et al. (2021). Frequency of deep-sea turbidity as an important component of the response of a source-to-sink system to climate: A case study in the eastern middle Bengal fan since 32 ka. *Mar. Geology* 441, 1–13. doi: 10.1016/j.margeo.2021.106603

Liu, J. P., Liu, C. S., Xu, K. H., Milliman, J. D., Chiu, J. K., Kao, S. J., et al. (2008). Flux and fate of small mountainous rivers derived sediments into the Taiwan strait. *Mar. Geology* 256 (1), 65–76. doi: 10.1016/j.margeo.2008.09.007

Liu, S. F., Li, J. R., Zhang, H., Cao, P., Mi, B. B., Khokiattiwong, S., et al. (2020). Complex response of weathering intensity registered in the Andaman Sea sediments to the Indian summer monsoon over the last 40 kyr. *Mar. Geology* 425, 106206. doi: 10.1016/j.margeo.2020.106206

Liu, J. G., Yan, W., Chen, Z., and Lu, J. (2012). Sediment sources and their contribution along northern coast of the south China Sea: Evidence from clay minerals of surface sediments. *Continental Shelf Res.* 47 (10), 156–164. doi: 10.1016/j.csr.2012.07.013

Liu, S. F., Ye, W. X., Cao, P., Zhang, H., Chen, M. T., Li, X. Y., et al. (2021a). Paleoclimatic responses to the tropic Indian ocean to regional monsoon and global climate change over the last 42 kyr. *Mar. Geology* 438, 1062542. doi: 10.1016/j.margeo.2021.106542

Liu, S. F., Ye, W. X., Chen, M. T., Pan, H. J., Cao, P., Zhang, H., et al. (2021b). Millennial-scale variability of Indian summer monsoon during the last 42 kyr: Evidence based on foraminiferal Mg/Ca and oxygen isotope records from the central bay of Bengal. *Palaeogeography Palaeoclimatology Palaeoecol.* 562, 110112. doi: 10.1016/j.palaeo.2020.110112

Manville, V., Németh, K., and Kano, K. (2009). Source to sink: a review of three decades of progress in the understanding of volcaniclastic processes, deposits, and hazards. *Sedimentary Geology* 220 (3), 136–161. doi: 10.1016/j.sedgeo.2009.04.022

McManus, J. (1988). "Grain size determination and interpretation," in *Techniques in sedimentology* (New Jersey: Blackwell Publishing).

Phillips, S. C., Johnson, J. E., Underwood, M. B., Guo, J., Giosan, L., and Rose, K. (2014). Long time scale variation in bulk and clay mineral composition of Indian continental margin sediments in the bay of Bengal, Arabian Sea, and Andaman Sea. *Mar. Petroleum Geology* 58, 117–138. doi: 10.1016/j.marpetgeo.2014.06.018

Qiao, S. Q., Shi, X. F., Fang, X. S., Liu, S. F., Kornkanitnan, N., Gao, J. J., et al. (2015). Heavy metal and clay mineral analyses in the sediments of upper gulf of Thailand and their implications on sedimentary provenance and dispersion pattern. *J. Asian Earth Sci.* 114, 488–496. doi: 10.1016/j.jseaes.2015.04.043

Rasmussen, S. O., Andersen, K. K., Svensson, A. M., Steffensen, J. P., Vinther, B. M., Clausen, H. B., et al. (2006). A new Greenland ice core chronology for the last glacial termination. *J. Geophysical Res.* 111, D06102. doi: 10.1029/2005JD006079

Reimer, P. J., Bard, E., Bayliss, A., Beck, J. W., Blackwell, P. G., Ramsey, C. B., et al. (2013). Selection and treatment of data for radiocarbon calibration: An update to the international calibration (IntCal) criteria. *Radiocarbon* 55, 23. doi: 10.2458/azu_js_rc.55.16955

Rodolfo, K. S. (1969). Sediments of the Andaman basin, northeastern Indian ocean. *Mar. Geology* 7 (5), 371–402. doi: 10.1016/0025-3227(69)90014-0

Sarin, M. M., Krishnaswami, S., Dilli, K., Somayajulu, B. L. K., and Moore, W. S. (1989). Major ion chemistry of the ganga-Brahmaputra river system: Weathering processes and fluxes to the bay of Bengal. *Geochimica Cosmochimica Acta* 53 (5), 997–1009. doi: 10.1016/0016-7037(89)90205-6

Sebastian, T., Nath, B. N., Miriyala, P., Linsy, P., and Kocherla, M. (2023). Climatic control on detrital sedimentation in the continental margin off chennai, western bay of Bengal-a 42 kyr record. *Palaeogeography Palaeoclimatology Palaeoecol.* 609, 111313. doi: 10.1016/j.palaeo.2022.111313

Selvaraj, K., and Chen, C. T. A. (2006). Moderate chemical weathering of subtropical Taiwan: Constraints from solid-phase geochemistry of sediments and sedimentary rocks. *J. Geology* 114, 101–116. doi: 10.1086/498102

Shi, X. F., Liu, S. F., Fang, X. S., Qiao, S. Q., Khokiattiwong, S., and Kornkanitnan, N. (2015). Distribution of clay minerals in surface sediments of the western gulf of Thailand: sources and transport patterns. *J. Asian Earth Sci.* 105, 390–398. doi: 10.1016/j.jseaes.2015.02.005

Shi, X. F., Qiao, S. Q., Yang, S. Y., Li, J. R., Wan, S. M., Zou, J. J., et al. (2021). Progress in sedimentology research of the Asian continental margin, (2011-2020). *Bull. Mineralogy Petrology Geochemistry* 40 (2), 319–336. doi: 10.3969/j.issn.1007-2802.2015.05.003

Sun, X. Q., Liu, S. F., Fang, X. S., Li, J. R., Cao, P., Zhao, G. T., et al. (2020). Clay minerals of surface sediments from the lower Bengal fan: Implications for provenance identification and transport processes. *Geological J.* 55 (9), 6038–6048. doi: 10.1002/gj.3786

Sun, X. Q., Liu, S. F., Li, J. R., Zhang, H., Zhu, A. M., Cao, P., et al. (2019). Major and trace element compositions of surface sediments from the lower Bengal fan: Implications for provenance discrimination and sedimentary environment. *J. Asian Earth Sci.* 184, 104000. doi: 10.1016/j.jseaes.2019.104000

Tripathy, G. R., Singh, S. K., Bhushan, R., and Ramaswamy, V. (2011). Sr-Nd Isotope composition of the bay of Bengal sediments: Impact of climate on erosion in the himalaya. *Geochemical J.* 45, 175–186. doi: 10.2343/geochemj.1.0112

Tripathy, G. R., Singh, S. K., and Ramaswamy, V. (2014). Major and trace element geochemistry of bay of Bengal sediments: Implications to provenances and their controlling factors. *Palaeogeography Palaeoclimatology Palaeoecol.* 397 (1), 20–30. doi: 10.1016/j.palaeo.2013.04.012

Waelbroeck, C., Labeyrie, L., Michel, E., Duplessy, J. C., McManus, J., Lambeck, K., et al. (2002). Sea-Level and deep water temperature changes derived from benthic foraminifera isotopic records. *Quaternary Sci. Rev.* 21, 295–305. doi: 10.1016/S0277-3791(01)00101-9

Weber, M. E., and Reilly, B. T. (2018). Hemipelagic and turbiditic deposits constrain lower Bengal fan depositional history through pleistocene climate, monsoon, and sea level transitions. *Quaternary Sci. Rev.* 199, 159–173. doi: 10.1016/j.quascirev.2018.09.027

Weber, M. E., Wiedicke, M. H., Kudrass, H. R., and Erlenkeuser, H. (2003). Bengal Fan sediment transport activity and response to climate forcing inferred from sediment physical properties. *Sedimentary Geology* 155, 361–381. doi: 10.1016/S0037-0738(02)00187-2

Xu, Z. K., Li, T. G., Chang, F. M., Wan, S. M., Choi, J., and Lim, D. (2014). Clay-sized sediment provenance change in the northern Okinawa trough since 22 kyr BP and its paleoenvironmental implication. *Palaeogeography Palaeoclimatology Palaeoecol.* 399 (2), 236–245. doi: 10.1016/j.palaeo.2014.01.016

Yang, S. Y., Wei, G. J., and Shi, X. F. (2015). Geochemical approaches of tracing source-to sink sediment process and environmental changes at the east Asian continental margin. *Bull. Mineralogy Petrology Geochemistry* 34 (5), 902–910.

Ye, W. X., Liu, S. F., Fan, D. J., Zhang, H., Cao, P., Pan, H.-J., et al. (2022). Evolution of sediment provenances and transport processes in the central bay of Bengal since the last glacial maximum. *Quaternary Int.* 629, 27–35. doi: 10.1016/j.quaint.2020.12.007